Int. J Solids Structures Vol 23, No 2, pp 211-237, 1987
Printed in Great Britain

0020-7683/87 $3.00+.00
Pergamon Journals Ltd.

A THEORY FOR DYNAMIC COMPACTION OF WET POROUS SOLIDS†

D. S. DRUMHELLER
Thermomechanical and Physical Division, Sandia National Laboratories, Alburquerque, NM 87185, U.S.A.

(*Received* 3 *July* 1985; *in revised form* 3 *February* 1986)

Abstract—Partially-saturated porous media exhibit complex behavior including plastic distortion, irreversible crushing of pores, and dilatancy. Pressure produced by compression of the pore fluid has a strong influence on these phenomena and greatly alters the response observed in the wet solid from that observed in the dry solid. This paper describes these phenomena within the framework of a theory for immiscible mixtures. It shows how a material representation originally derived for the hydrostatic compaction of a dry solid can be generalized to wet solids subjected to both distortional and volumetric deformation. Results of stress-wave calculations are compared to data obtained from a field test in which high explosive was detonated in a formation of partially-saturated ashfall tuff.

1. INTRODUCTION

The compressive response of a porous solid, either partially or totally saturated with a fluid, poses an interesting and formidable problem in the constitutive characterization of mixtures. Rock saturated with water is a particular example which has received wide attention. The work of Terzaghi[1] is a classical example of an early attempt to account for the effects of fluid pressure acting within the pores of a rock matrix. In this case an effective stress for the solid was evaluated by subtracting the pore pressure from the total pressure applied to the rock–water mixture. Thus it was supposed that the pore pressure aids the rock matrix in supporting the total load and correspondingly reduces the effective load on the matrix.

Within the framework of mixture theory, Terzaghi's effective-stress principle constitutes a *mixing rule* linking together the deformations and loads intrinsic to each of the constituents. Ideally, mixing rules are used to quantify the particular microstructure existing in the mixture. For example, they might account for the differences between two types of rock, each composed of the same mineral, one containing spherical pores and the other containing penny-shaped cracks. The process by which constitutive principles for simple continua are established is difficult enough; however, the additional complication of determining mixing rules for mixture continua has severely limited solutions to practical problems for fluid-saturated rock in particular and for structured mixtures in general[2].

Motivated by the practical importance of this problem, several authors have elaborated and improved upon Terzaghi's original efforts. Biot and Willis[3] and later Nur and Byerlee[4] proposed a modification to the effective stress rule. Nur and Byerlee's paper clearly identifies the problem inherent with Terzaghi's original rule. They point out that the kinematics of the deformation of the solid matrix involves both a gross motion of the solid matrix and a local motion associated with changes in the pore volume. They argue that if the intrinsic pressures of the solid and the fluid are increased an equal amount, the fraction of the total volume occupied by the solid will not change. This observation gives rise to a new mixing rule where only a fraction of the pore pressure is subtracted from the total pressure to arrive at the effective pressure on the solid. The fraction is given by the expression $(1 - K/K_s)$ where K and K_s represent the bulk moduli of the dry porous solid and the fully compacted or non-porous solid. Most recently Carroll and Katsube[5] have extended this idea to more complex kinematics associated with anisotropic elastic materials.

†This work was performed at Sandia National Laboratories and supported by the U.S. Department of Energy under contract No. DE-AC04-76DP00789.

The work of Biot and Willis was motivated by an earlier work of Biot[6], wherein he did not include the kinematics necessary to arrive at the modification of Terzaghi's effective stress rule. In that paper Biot assumed that the effective stress in the solid was a function of the gross deformation of the solid and not a function of the volume fraction of the solid. Some years later Bedford and Drumheller[7] proposed a related theory wherein this expanded functional dependence was included. In this paper they demonstrated the relationship of their work to Biot's earlier theory. In a still later work Bedford and Stern[8] extended this work to sediments containing both gases and liquids.

The approach adopted by Bedford and Drumheller was to study this problem within the framework of the continuum theory of mixtures. In particular they used a theory specialized to an immiscible mixture; that is, a mixture with internal microstructure, and one where the intrinsic properties of the constituents are still identifiable[2, 9]. Other authors have also adopted this type of approach. In earlier works, Morland[10], Garg[11], and Garg and Nur[12] proposed a model for a fluid-saturated porous solid based on a more general mixture theory not specialized to immiscible mixtures. This mixture theory was modified to include the intrinsic behaviors for each of the constituents. The partial mass densities and partial stresses appearing in the mixture continuum equations were related to the intrinsic behavior through a set of constitutive equations for the volume fractions of the constituents. Thus the mixing rules were expressed as relations linking the volume fractions of the constituents to other kinematical quantities in the theory.

In this paper the behavior of a rock–water system will be studied using the immiscible mixture theory proposed by Drumheller and Bedford[9]. This theoretical framework is useful for two important reasons. First, the theory has been specialized to immiscible mixtures. Thus the intrinsic properties of the constituents such as the mass densities are readily available in the theory. Second, the thermodynamics of the mixture are clearly defined including the energy balance equations and the implications of the second law of thermodynamics.

The problem under consideration requires the computation of shock waves in a partially-saturated tuff. The shock waves are generated by the detonation of a spherical charge of high explosive buried in the tuff. This charge contains about 900 kg of material and produces pressures in the tuff of the order of 10 GPa. Effects of the detonation range radially outward for about 20 m. The field experiment was performed under the direction of Smith[13]. Numerous accelerometers and stress gages recorded the shock wave as it propagated through the tuff. Pressures and displacements within the explosively-formed underground cavity were also measured.

While the early-time response of the wet tuff requires the computation of large-amplitude stress waves, the late-time response, which determines the final cavity radius, is dominated by low pressures of the order of the strength of the tuff (in the range of 0.01–0.1 GPa). Consequently both high-pressure effects dominated by shock-heating phenomena and low-pressure effects dominated by material-strength phenomena are present in this problem. Varying amounts of pore collapse occur depending upon the distance from the detonation site, and after the detonation the final saturation levels in the tuff vary.

This experiment was performed primarily to investigate the formation of a *stress cage*. This is an annular region about the detonation cavity containing residual compressive stresses. These radial and hoop stresses are thought to form because of the divergent nature of the spherical shock waves in combination with large plastic deformations. One of the purposes of the calculations presented here is to study the formation of the stress cage and to predict the residual pressure field in the pore fluid.

Since much of this problem is dominated by the shock wave response of the wet tuff, the theoretical development will be directed towards the incorporation of conventional methods of shock wave analysis for single continua into a multiple or mixture continuum framework. The intrinsic response of tuff and water will be formulated with the Mie–Grüneisen model which historically has proven very useful[14]. Also, the mixing rule for the mechanical coupling between the constituents will be extracted from previous shock wave studies.

To the reader familiar with shock wave work this last statement may be somewhat surprising, since mixing rules apparently have not received significant attention in this field. However, as shown here, an earlier modeling study on dry porous materials can be extended to produce a mixing rule appropriate to the current problem. This is the P–α model of Herrmann[15]. In Herrmann's formulation the volume fraction of the solid is linked through the P–α function to the intrinsic pressure in the solid. If the argument of this function is changed from the intrinsic pressure in the solid to the pressure difference between the solid and the pore fluid, it will be shown that the P–α function also describes the behavior of a wet solid. This conclusion, which is an extension of the original observation of Nur and Byerlee, will be derived from the basic principles connected to the first and second law of thermodynamics. Furthermore, these principles will be used to extend the P–α function to include distortional effects which manifest themselves through the phenomena of dilatancy.

In Sections 2 and 3 a theory for a partially-saturated porous solid is derived and specialized to an ashfall tuff containing water. Section 4 describes the field experiment where this material was subjected to a dynamic compaction generated by a buried charge of TNT. This section also contains a set of material parameters appropriate to this problem. Section 5 describes the numerical methods used to model this experiment, and Section 6 discusses the results of the calculation and compares them to the test data.

2. THEORY

To anyone who has read some part of the literature on mixture theory, it is apparent these papers can be categorized into two broad classes, applications papers and theoretical expositions. Both groups serve a useful purpose; however, each has its limitations. The applications papers usually present an *ad hoc* theory designed to solve a specific problem. They are limited in their scope to that problem alone and may prove insufficient when applied to other problems. For example, many are limited to one-dimensional problems and cannot easily be generalized to two- or three-dimensional problems. At the other extreme, the theoretical expositions are usually quite complicated and are often difficult to relate to practical applications.

Until recently, this split was natural since the general principles of mixture theory were in a state of flux and anyone wishing to actually solve a problem had to turn to other means. Fortunately this situation has changed in the past few years and the continuum mechanics approach to mixture theory offers a useful and powerful tool for solving a variety of practical problems. The key to this change is a specialization of general mixture theory to problems dealing with immiscible mixtures; that is, mixtures which appear heterogeneous on some microscale. Dusty gases, bubbly liquids and fluid-saturated porous solids are good examples of these types of mixtures.

This specialization is an important step allowing for the introduction of the concept of intrinsic material properties. Thus in a mixture of a fluid and a solid, the constitutive properties of the pure fluid and the pure solid can be used to construct constitutive properties for the solid–fluid mixture. The resulting theory contains not only the partial mass density of each constituent but also its intrinsic mass density.

Theories which result from this type of approach still require specification of mixing rules linking the constitutive behaviors of each constituent together; however, in many cases simple mixing rules are sufficient for a wide variety of problems. Quite useful theories can be derived by assuming such simple mixing rules as pressure and temperature equilibrium between the constituents.

In cases requiring more complex mixing rules, the necessary information may already be available from previous studies. The present work is a good example. This work will require a mixing rule for a porous solid and a fluid. Over the range of pressures to be considered, an equal-pressure mixing rule is not adequate since the solid has sufficient strength to support a load and not crush completely even when no pore fluid is present.

Previous studies on dry porous materials have resulted in a variety of theories to describe this crush-up behavior. One notable theory is the P–α model of Herrmann[15]. It will be shown that this model, originally derived for a dry solid, is also a mixing rule describing the behavior of the solid under all saturation conditions.

With the exception of the constitutive equations, the theory necessary to describe the present problem is given in Ref. [9] which contains a detailed description of the kinematics of the problem and a development of the balance equations of mass, momentum and energy. This work also contains the important development of the constitutive restrictions arising from the entropy inequality of the second law of thermodynamics. These results are far more complex than required here, since they apply to problems with material diffusion and chemical reactions. It will be assumed here that the porous solid and the pore fluid have identical motions and do not exchange mass. This simplification greatly facilitates the derivation of the balance equations. Because of this, and for the sake of completeness and clarity, the balance equations will be derived in this work. Not all of the points of the derivation will be covered in detail. The reader is advised to consult Ref. [9] for these details.

The theoretical development will be presented out of the traditional order in that the constitutive description will be introduced before the derivation of the balance equations for momentum and energy. This is done to help motivate the definitions of many of the terms appearing in these balance equations. However, the derivation will still begin with a description of the kinematics of the problem.

Because material diffusion; that is, relative motion between the constituents, will not be considered, the mixture motion can be described by a single vector function. The original or reference position of an element of the mixture is denoted by the vector X_i, where the index i assumes integer values of 1, 2 and 3. The current position of this element is denoted by x_i. If the parameter t represents time, then

$$x_i = \chi_i(X_j, t). \tag{1}$$

The velocity and acceleration of this element of the mixture are given as

$$v_i = \frac{\partial}{\partial t}\chi_i(X_j, t) \tag{2}$$

and

$$a_i = \frac{\partial^2}{\partial t^2}\chi_i(X_j, t). \tag{3}$$

The Jacobian of the deformation of this element is given as

$$J = \det\left[\frac{\partial}{\partial X_j}\chi_i(X_j, t)\right]. \tag{4}$$

Another useful definition, the velocity gradient, is

$$\mathscr{L}_{ij} = \frac{\partial v_i}{\partial x_j}. \tag{5}$$

For convenience the ξth constituent of the mixture is referred to as C_ξ. The partial mass density of C_ξ is denoted by ρ_ξ. Within an elemental volume of the mixture, this is the ratio of the mass of C_ξ over the total volume. The intrinsic mass density of C_ξ is denoted by $\bar{\rho}_\xi$. This is the ratio of the mass of C_ξ over the portion of the volume occupied

by C_ξ. The partial mass density and the intrinsic mass density are related through the volume fraction ϕ_ξ

$$\rho_\xi = \phi_\xi \bar{\rho}_\xi. \tag{6}$$

The introduction of the intrinsic mass density is central to this theory. For example, consider the point that the pressure in the pore fluid is most naturally written as a function of the intrinsic and not the partial mass density.

Each constituent obeys a balance of mass relation expressed as (see Ref. [9])

$$\rho_\xi J = \rho_{\xi 0} \tag{7}$$

where the zero subscript denotes a reference value. This relation can also be expressed in an equivalent differential form as

$$\dot{\rho}_\xi + \rho_\xi \frac{\partial v_i}{\partial x_i} = 0 \tag{8}$$

where summation on repeated indices is implied and where the material derivative of ρ_ξ is given by

$$\dot{\rho}_\xi = \frac{\partial \rho_\xi}{\partial t} + v_i \frac{\partial \rho_\xi}{\partial x_i}.$$

The mixture mass density ρ is related to the constituent mass densities by the relation

$$\rho = \sum \rho_\xi \tag{9}$$

where the summation sign implies a summation over all C_ξ. By summing eqn (7) over all C_ξ and using eqn (9), the balance of mass relation for the mixture is found to be

$$\rho J = \rho_0. \tag{10}$$

Obviously it is important to obtain mixture balance laws which are identical to the balance laws for a single continuum. In part, the motivation for the definition of ρ in eqn (9) is to ensure the form of eqn (10). Similar definitions of mixture stresses, energy, etc. are used to ensure the recovery of the single-continuum balance laws for momentum and energy.

Another useful definition is the mass fraction γ_ξ of C_ξ given by

$$\gamma_\xi = \frac{\rho_\xi}{\rho} = \frac{\rho_{\xi 0}}{\rho_0}. \tag{11}$$

Here eqns (7) and (10) have been used to show that the γ_ξs are constants due to the omission of relative motion between the C_ξs.

The final point to be discussed with regard to the kinematics of this problem is the saturation condition on the volume fractions

$$\sum \phi_\xi = 1. \tag{12}$$

We will consider this mixture to be composed of three constituents: porous solid, pore fluid, and void. Consequently, when the solid is only partially saturated with fluid, the volume fraction of the void will be nonzero.

Before the balance laws for momentum can be presented, the types of forces resulting in motion within the mixture must be defined. It is assumed the pore fluid can only exert a pressure. The constitutive relation for this constituent will relate the pressure in the fluid to its intrinsic mass density and its temperature. The forces present in the porous solid, however, are more complex.

It was pointed out by Bedford and Drumheller[7] that two types of loads exist in the porous solid. Obviously, the solid must interact through one type of load with the pore fluid. However, this is not the only load in the solid, since when the pore fluid is absent, the pores in the solid do not automatically collapse. The solid still retains the ability to support a configurational load which ensures the existence of a finite amount of porosity in the dry solid provided that the magnitudes of the applied loads are not too high. Contrast this behavior with that of the fluid, if the solid is extracted from the mixture. Voids left behind by the removal of the solid will be filled immediately upon loading, because the fluid cannot support a similar configurational load.

As an additional example of the behavior of the solid, consider the situation when the solid fills a rigid container. If the pore pressure were changed by pumping additional fluid into the solid, then the intrinsic mass density of the solid would change but the partial mass density would remain fixed. Other experiments could be performed to change the partial mass density but not the intrinsic mass density. Entirely different loads would have to be used to achieve each of these situations.

These examples illustrate that the response of the solid must be represented by several types of loads, each of which act through their complementary motions, in this case local motions associated with changes in the intrinsic mass density and the gross motion, eqn (1). For single constituent continua when a void is not present, the intrinsic mass density is kinematically coupled to the motion through the balance of mass relation and this separation of the loads is not necessary; however, when a void or another constituent is present this coupling does not exist.

The equilibrium response of a material can be described by a thermodynamic potential function. In this work two potential functions will be defined; one for the solid and one for the pore fluid. As an introduction to these definitions, some points are worth noting about potential functions for conventional continua.

The response of a fluid can be described by the expression for the Helmholtz free energy $\Psi_f = \hat{\Psi}_f(\rho_f, \theta_f)$ where θ_f is the absolute temperature. This energy function does not depend on the distortion of the material, and therefore the fluid will not support shear loads at equilibrium. For a solid, the potential function is more complicated; for example, $\Psi_s = \hat{\Psi}_{sb}(\rho_s, \theta_s) + \hat{\Psi}_{sg}(\Lambda, \theta_s)$. In this case the deformation of the material is divided into spherical and distortional components. The measure of the spherical component of deformation is the mass density ρ_s, and the measure of the distortional, or shearing, component is the magnitude of the deviator strain represented by Λ. Consequently the first term in this expression represents the mean stress or pressure response, and the second term represents the deviatoric or shearing response.

Since the spherical and distortional energies have been specified through separate additive terms, this potential function is not the most general representation of a solid. This separation results in an equilibrium response in which the pressure and the shear stresses are uncoupled; that is, pure distortion does not result in a change in pressure, and compression does not alter the shear stresses or the shear modulus. This is a common assumption in many theories for solids and will be adopted here for the intrinsic response of the mineral forming the matrix of the porous solid.

The required potential functions for the mixture constituents are modifications of these relations. The required function for the pore fluid is easily obtained by distinguishing between its partial mass density and its intrinsic mass density so that

$$\Psi_f = \hat{\Psi}_f(\bar{\rho}_f, \theta_f). \tag{13}$$

This implies that the behavior of the fluid is not altered by its introduction into the pores of the solid.

In contrast, the solid behavior is altered by the presence of the pores. The energy state of the solid will depend on the volume fraction of the solid as well as the intrinsic mass density. The philosophy in this case is to minimize the complexity of the alteration of this energy function while retaining sufficient generality to model the physical phenomena. Thus to model the effect of distention on the bulk or spherical response of the solid, an arbitrary function of the volume fraction of the solid will be added to $\hat{\Psi}_{sb}$. Similarly to model the effect of distention on the distortional response, an arbitrary function of the volume fraction will be multiplied with $\hat{\Psi}_{sg}$. The resulting expression for the distended solid is

$$\Psi_s = \hat{\Psi}_{sb}(\bar{\rho}_s, \theta_s) + \hat{g}(\tilde{\phi}_s)\hat{\Psi}_{sg}(\Lambda, \theta_s) + \hat{F}(\tilde{\phi}_s). \tag{14}$$

Because large amounts of plastic deformation will occur in the solid, the volume fraction of the solid has been separated into an elastic and a plastic part. The elastic part of the volume fraction of the solid is denoted by $\tilde{\phi}_s$. Similarly Λ is related to the elastic distortion associated with the motion, eqn (1), as follows: when elastic motions occur the elastic strain is defined by the strain-rate

$$\dot{\varepsilon}_{ij} = \frac{1}{2}(\mathscr{L}_{ij} + \mathscr{L}_{ji}); \tag{15}$$

given that the deviator components of the elastic strain are

$$\varepsilon'_{ij} = \varepsilon_{ij} - \frac{1}{3}\varepsilon_{kk}\delta_{ij} \tag{16}$$

the second invariant of this tensor is

$$\Lambda = \varepsilon'_{ij}\varepsilon'_{ij}. \tag{17}$$

The free energy of the fluid is a function of the intrinsic mass density and the temperature alone. Conventional arguments of thermodynamics can be used to show that the fluid pressure P_f is related to the partial derivative of Ψ_f with respect to $\bar{\rho}_f$, and the entropy of the fluid S_f is related to the partial derivative with respect to θ_f. It will be shown that the partial derivatives of eqn (14) are also related to the pressure P_s which interacts with the pore fluid, the configurational stress T_{ij} which prevents the pores from closing in the absence of pore fluid, and the entropy S_s. It is also helpful to point out at this time that introduction of the function $\hat{g}(\tilde{\phi}_s)$ will result in the phenomena of dilatancy in the solid, and introduction of the function $\hat{F}(\tilde{\phi}_s)$ is equivalent to inclusion of a P–α curve for the solid[15].

Since each of the loads is related to a partial derivative of the appropriate free energy function, each of the loads must do work on the mixture when its complementary variable is varied. The balance of linear momentum for this mixture can be derived from a form of Hamilton's variational principle in which the virtual work of each of the loads is considered. The appropriate expression for the virtual work δW is

$$\delta W = \int_V \left\{ -T_{ij}\frac{\partial(\delta x_i)}{\partial x_j} - \phi_s P_s \frac{\delta\bar{\rho}_s}{\bar{\rho}_s} - \phi_f P_f \frac{\delta\bar{\rho}_f}{\bar{\rho}_f} + \rho f_i \delta x_i \right\} \mathrm{d}V. \tag{18}$$

The operator δ denotes the variation of the function, f_i represents a specific external body force such as gravity, and V denotes the current volume of the mixture. This relation stipulates that the configurational stress T_{ij} does work only when the deformation associated with the motion x_i changes. It also specifies that the P_ξs do work only when the intrinsic mass densities $\bar{\rho}_\xi$ change.

Hamilton's variational principle requires†

$$\delta\int_{t_1}^{t_2}\left\{\int_V\left[\frac{1}{2}\rho v_i v_i\right]\mathrm{d}V\right\}\mathrm{d}t+\int_{t_1}^{t_2}\left\{\delta W-\int_V\left[\lambda\delta\left(\sum\phi_\xi-1\right)\right.\right.$$
$$\left.\left.-\sum\mu_\xi\delta\left(J-\frac{\rho_{\xi 0}}{\rho_\xi}\right)\right]\mathrm{d}V\right\}\mathrm{d}t=0 \qquad (19)$$

where t_1 and t_2 are arbitrary times, and eqns (7) and (12) are included as constraints through the use of the Lagrange multipliers λ and μ_ξ.

By applying the variational techniques described by Drumheller and Bedford[9], this relationship can be rewritten as

$$\int_{t_1}^{t_2}\int_V\left\{-\rho a_i\delta x_i+\frac{\partial T_{ij}}{\partial x_j}\delta x_i-\sum\phi_\xi\rho_\xi\frac{\delta\bar{\rho}_\xi}{\bar{\rho}_\xi}-\lambda\sum\delta\phi_\xi\right.$$
$$\left.+\sum\left[\mu_\xi J\left(\frac{\delta\bar{\rho}_\xi}{\bar{\rho}_\xi}+\frac{\delta\phi_\xi}{\phi_\xi}\right)-\frac{\partial(\mu_\xi J)}{\partial x_i}\delta x_i\right]\right\}\mathrm{d}V\mathrm{d}t=0. \qquad (20)$$

In the problems of interest δx_i, $\delta\bar{\rho}_s$ and $\delta\bar{\rho}_f$ are nontrivial and arbitrary quantities. Thus the Euler–Lagrange conditions require that the coefficients of these quantities independently be set to zero. Thus

$$\rho a_i=\frac{\partial T_{ij}}{\partial x_j}-\frac{\partial}{\partial x_i}(\mu_f J+\mu_s J)+\rho f_i \qquad (21)$$

$$\mu_s J=\phi_s P_s \qquad (22)$$

and

$$\mu_f J=\phi_f P_f. \qquad (23)$$

The cases of interest will include a fully-compacted dry solid, a dry solid with void, a partially-saturated solid, and a fully-saturated solid. Thus ϕ_s, ϕ_f or ϕ_v could be constants. The appropriate Euler–Lagrange conditions for the associated terms in eqn (20) are:

either $\delta\phi_s=0$ or

$$\mu_s J=\lambda\phi_s; \qquad (24)$$

either $\delta\phi_f=0$ or

$$\mu_f J=\lambda\phi_f; \qquad (25)$$

and either $\delta\phi_v=0$ or

$$\lambda=0. \qquad (26)$$

† As explained in Ref. [9], use of Hamilton's variational principle in this form does *not* imply a conservative force system.

Examination of the above relations will show that an equivalent set of relations will satisfy all possible special cases of dry, partially-saturated, and fully-saturated mixtures. To illustrate this, solve eqns (22)–(25) to obtain

$$P_f = P_s = \lambda. \tag{27}$$

In the special case where voids exist; that is, if the solid is only partially-saturated with fluid, then $\delta\phi_v \neq 0$, and eqn (26) holds. Equations (22)–(25) then require $P_f = P_s = 0$. This is equivalent to requiring eqn (27) to hold with the additional stipulation, $\lambda = 0$. Next if void exists in the total absence of fluid, then $\delta\phi_f = 0$. Equations (22), (24) and (26) then require $P_s = 0$, and eqn (25) does not apply. Since $\phi_f = 0$, eqn (23) requires $\mu_f = 0$, and as a result P_f decouples from the system of equations. This is again equivalent to requiring eqn (27) to hold, and $\lambda = 0$. In the special case when the solid occupies all of the volume, eqns (24)–(26) do not apply. The variables P_s and λ completely decouple from the remaining equations, and eqn (27) becomes an extraneous relation. Finally, for the fully-saturated solid $\delta\phi_v = 0$, and eqn (26) does not apply. Again eqn (27) holds, and $\lambda \neq 0$. Therefore, eqn (27) applies to all possible cases provided $\lambda = 0$ when void is present.

By using eqns (22), (23) and (27) in eqn (21), the balance of the linear momentum relation becomes

$$\rho a_i = \frac{\partial}{\partial x_j}(T_{ij} - \lambda\delta_{ij}) + \rho f_i. \tag{28}$$

This relation has the familiar form of the Terzaghi effective stress theory[1]. However, in the effective stress theory it is usually assumed that the term T_{ij} is a function of the motion alone. This is not the case in the present work where T_{ij} also depends on the intrinsic mass density of the solid $\bar{\rho}_s$.

The virtual work statement, eqn (18), leads directly to the balance of energy equations for each C_ξ. By using the approach described by Drumheller and Bedford[9] and by ignoring heat conduction, the energy balance laws are

$$\rho_s \dot{E}_s = T_{ij}\mathscr{L}_{ij} + \phi_s P_s \frac{\dot{\bar{\rho}}_s}{\bar{\rho}_s} + \rho_s r_s + \dot{e}_s \tag{29}$$

and

$$\rho_f \dot{E}_f = \phi_f P_f \frac{\dot{\bar{\rho}}_f}{\bar{\rho}_f} + \rho_f r_f + \dot{e}_f \tag{30}$$

where E_ξ denotes the specific internal energy of C_ξ. The terms r_ξ and $\dot{e}_\xi$ represent the specific external heat supply and the energy production rate of C_ξ. These two terms denote energy contributions from outside sources such as electromagnetic radiation and energy exchange between the constituents due to local temperature differences. It is required that

$$\sum \dot{e}_\xi = 0. \tag{31}$$

The specific internal energy of the mixture and the specific external heat supply of the mixture are defined as

$$E = \sum \gamma_\xi E_\xi \tag{32}$$

and

$$r = \sum \gamma_\xi r_\xi. \tag{33}$$

Since by eqn (11) the γ_ξs are constants, the energy relations, eqns (29) and (30), can be summed to obtain

$$\rho \dot{E} = T_{ij} \mathscr{L}_{ij} + \lambda \frac{\dot{\rho}}{\rho} + \rho r \tag{34}$$

where eqns (6), (7), (12) and (27) have also been used.

The balance laws for mass, momentum and energy are now complete. The next step is to investigate the implications of the second law of thermodynamics. The production of entropy, S_ξ, within the mixture is required to satisfy the following inequality:

$$\sum \left(\rho_\xi \dot{S}_\xi - \frac{\rho_\xi}{\theta_\xi} r_\xi \right) \geqslant 0. \tag{35}$$

This relation will be viewed as a constraint upon the constitutive relations; that is, the constitutive relations will be specified by a method which guarantees that the inequality will always be satisfied. The procedure followed in this work is one originally proposed by Coleman and Noll[16]. The present concern is to produce constitutive relations for the mixture constituents which are sufficient but not necessary to satisfy inequality (35) while retaining enough generality for use in the immediate application and in similar applications.

The Helmholtz free energy Ψ_ξ, specific internal energy E_ξ, and the entropy S_ξ are connected through the definition

$$\Psi_\xi = E_\xi - S_\xi \theta_\xi. \tag{36}$$

This expression can be differentiated and substituted into inequality (35). The energy relations, eqns (29) and (30), can also be solved for the r_ξs and substituted into inequality (35). The resulting expression will contain the time derivatives of Ψ_ξ which can be expressed in a chain-rule expansion by using eqns (13) and (14). These manipulations produce the following result:

$$\begin{aligned} &- \sum \left[\frac{\rho_\xi}{\theta_\xi} \left(S_\xi + \frac{\partial \Psi_\xi}{\partial \theta_\xi} \right) \right] \dot{\theta}_\xi + \sum \frac{\dot{e}_\xi}{\theta_\xi} \\ &+ \sum \left[\frac{\phi_\xi}{\theta_\xi} \left(P_\xi - \bar{\rho}_\xi^2 \frac{\partial \Psi_\xi}{\partial \bar{\rho}_\xi} \right) \frac{\dot{\bar{\rho}}_\xi}{\bar{\rho}_\xi} \right] \\ &+ \frac{1}{\theta_s} \left[T_{ij} \mathscr{L}_{ij} - \rho_s \frac{\partial \Psi_s}{\partial \varepsilon'_{ij}} \dot{\varepsilon}'_{ij} - \rho_s \frac{\partial \Psi_s}{\partial \phi_s} \dot{\phi}_s \right] \geqslant 0. \end{aligned} \tag{37}$$

This inequality is based only on the constitutive assumptions for the Helmholtz free energies, eqns (13) and (14). The functional dependence of the remaining constitutive assumptions must be specified before the analysis can proceed. It will be assumed

$$S_f = \hat{S}_f(\bar{\rho}_f, \theta_f) \tag{38}$$

$$S_s = \hat{S}_s(\bar{\rho}_s, \varepsilon_{ij}, \theta_s) \tag{39}$$

$$P_f = \hat{P}_f(\bar{\rho}_f, \theta_s) \tag{40}$$

$$P_s = \hat{P}_s(\bar{\rho}_s, \varepsilon_{ij}, \theta_s) \tag{41}$$

$$T_{ij} = \hat{T}^e_{ij}(\bar{\rho}_s, \varepsilon_{ij}, \theta_s) + \hat{T}^d_{ij}(\bar{\rho}_s, \varepsilon_{ij}, \theta_s, \dot{\bar{\rho}}_s, \dot{\varepsilon}_{ij}) \tag{42}$$

and

$$\dot{e}_\xi = \hat{\dot{e}}_\xi(\bar{\rho}_\zeta, \varepsilon_{ij}, \theta_\zeta). \tag{43}$$

These statements embody what is called the immiscibility assumption. It is assumed that the intrinsic loads acting on C_ξ depend only on the intrinsic properties of C_ξ, while the interactive quantities, in this case $\dot{e}_\xi$, depend on the parameters of all of the constituents. Two other points should also be noted. First, since C_j is a fluid, its behavior does not depend on ε_{ij}. Second, the configurational stress tensor has been divided into an equilibrium and a dissipative part. The dissipative component of T_{ij} is included because solutions to shock phenomena will be required.† It is assumed at equilibrium, when $\dot{\bar{\rho}}_s$ and $\dot{\varepsilon}_{ij}$ are zero, the term T^d_{ij} is also zero.

Returning to the inequality, the arguments originally presented by Coleman and Noll can be used to establish additional constraints on these assumptions. It is assumed the functional forms of the constitutive assumptions must guarantee that the inequality will always be satisfied. Since $\dot{\theta}_\xi$ does not appear in the list of independent variables of the constitutive assumptions, it can be argued that the coefficients of these terms in the inequality must be set to zero. Thus

$$S_\xi = -\frac{\partial \Psi_\xi}{\partial \theta_\xi}. \tag{44}$$

Similarly, since $\dot{\bar{\rho}}_f$ appears in the third term of inequality (37) and nowhere else

$$P_f = \bar{\rho}_\xi^2 \frac{\partial \Psi_\xi}{\partial \bar{\rho}_\xi}. \tag{45}$$

The stress tensor T_{ij} is assumed to be symmetric. It is convenient to define the deviatoric components T'_{ij}

$$T'_{ij} = T_{ij} - \frac{1}{3} T_{kk} \delta_{ij}. \tag{46}$$

† Shock waves are steady waves with extremely rapid rise times. They exist because the non-linear response of a material causes a compression wave to continue to "shock up" until the dissipative forces of the material limit any further sharpening of the wave[17]. In computer codes designed to handle these types of problems, these dissipative forces are usually lumped into an "artificial-viscosity" term which is proportional to either the first or second power of the strain rate[18]. These terms are designed to have negligible effects on the solution at points where shock waves do not exist. For this reason a dissipative term has been included in the expression for T_{ij}. This implies the dissipative forces reside solely in the solid matrix, which is a reasonable approximation considering the granular nature of the material. The physical intent of this assumption is to approximate a phenomenon resulting in *shock heating*, the production of entropy during passage of a shock wave. In practice this assumption is used to "stabilize" numerical solutions.

By using the above results and definitions, the entropy inequality reduces to

$$\frac{1}{\theta_s}\left[\frac{1}{2}T'_{ij}(\mathscr{L}_{ij}+\mathscr{L}_{ji})-2\rho_s g\frac{\partial\Psi_{sb}}{\partial\Lambda}\varepsilon'_{ij}\dot{\varepsilon}'_{ij}\right]$$
$$-\frac{1}{\theta_s}\left[\frac{1}{3}T_{kk}\frac{\dot{\phi}_s}{\phi_s}+\left(\phi_s\rho_s\frac{\partial g}{\partial\tilde{\phi}_s}\Psi_{sg}+\phi_s\rho_s\frac{\partial E}{\partial\tilde{\phi}_s}\right)\frac{\dot{\tilde{\phi}}_s}{\phi_s}\right]$$
$$-\frac{1}{\theta_s}\left[\frac{1}{3}T_{kk}-\phi_s P_s+\phi_s\bar{\rho}_s^2\frac{\partial\Psi_{sb}}{\partial\bar{\rho}_s}\right]\frac{\dot{\bar{\rho}}_s}{\bar{\rho}_s}$$
$$+\sum\frac{\dot{e}_\xi}{\theta_\xi}\geqslant 0. \tag{47}$$

It is now argued that the inequality is at its minimum value and equal to zero at equilibrium. In the neighborhood of equilibrium eqn (15) holds and $\dot{\phi}_s=\dot{\tilde{\phi}}_s$. Under these circumstances the coefficients of $\dot{\varepsilon}'_{ij}$, $\dot{\phi}_s$ and $\dot{\bar{\rho}}_s$ must be zero. Since by definition T^d_{ij} is also zero at equilibrium

$$T^{e'}_{ij}=2\rho_s g\frac{\partial\Psi_{sg}}{\partial\Lambda}\varepsilon'_{ij} \tag{48}$$

$$\frac{1}{3}T^e_{kk}=-\phi_s\rho_s\frac{\partial g}{\partial\tilde{\phi}_s}\Psi_{sg}-\phi_s\rho_s\frac{\partial F}{\partial\tilde{\phi}_s} \tag{49}$$

and

$$P_s=\bar{\rho}_s^2\frac{\partial\Psi_{sb}}{\partial\bar{\rho}_s}-\rho_s\frac{\partial g}{\partial\tilde{\phi}_s}\Psi_{sg}-\rho_s\frac{\partial F}{\partial\tilde{\phi}_s}. \tag{50}$$

By using these relations, the inequality now reduces to

$$\frac{1}{\theta_s}\left\{T^{e'}_{ij}\left[\frac{1}{2}(\mathscr{L}_{ij}+\mathscr{L}_{ji})-\dot{\varepsilon}'_{ij}\right]-\frac{1}{3}T^e_{kk}\left(\frac{\dot{\phi}_s}{\phi_s}-\frac{\dot{\tilde{\phi}}_s}{\phi_s}\right)\right\}$$
$$+\frac{1}{\theta_s}\left\{-\frac{1}{3}T^d_{kk}\frac{\dot{\rho}_s}{\rho_s}+\frac{1}{2}T^{d'}_{ij}(\mathscr{L}_{ij}+\mathscr{L}_{ji})\right\}+\sum\frac{\dot{e}_\xi}{\theta_\xi}\geqslant 0. \tag{51}$$

This reduced inequality will be satisfied by writing relations for $\dot{\varepsilon}'_{ij}$, $\dot{\tilde{\phi}}_s$, $\dot{e}_\xi$, and T^d_{ij} to ensure each of the terms in inequality (51) individually satisfies the inequality.

3. CONSTITUTIVE MODEL FOR WET TUFF

Solutions to problems involving large amplitude wave propagation in solids can normally be accomplished with theories having incomplete thermodynamic descriptions. For the present problem, the Mie–Grüneisen formalism[14] will be used to represent the intrinsic behavior of the constituents. In this formalism the pressures are written as functions of the intrinsic mass densities and the specific internal energies. In other parts of the constitutive equations the dependence on thermal quantities will also be minimized. For example, it has already been assumed that the functions $\hat{F}(\tilde{\phi}_s)$ and $\hat{g}(\tilde{\phi}_s)$ do not depend on temperature.

If the pressure due to the intrinsic bulk response of the solid is denoted as P_{sb} where

$$P_{sb} = \bar{\rho}_s^2 \frac{\partial \Psi_{sb}}{\partial \bar{\rho}_s} \tag{52}$$

the Mie–Grüneisen approximations to the intrinsic material response of the solid, eqn (52), and the fluid, eqn (45), are

$$P_f = \frac{\bar{\rho}_{f0} c_{f0}^2 \eta_f}{(1 - s_f \eta_f)^2}\left[1 - \frac{\Gamma_f}{2}\left(\frac{\bar{\rho}_f}{\bar{\rho}_{f0}} - 1\right)\right] + \Gamma_f \bar{\rho}_f E_f \tag{53}$$

and

$$P_{sb} = \frac{\bar{\rho}_{s0} c_{s0}^2 \eta_s}{(1 - s_s \eta_s)^2}\left[1 - \frac{\Gamma_s}{2}\left(\frac{\bar{\rho}_s}{\bar{\rho}_{s0}} - 1\right)\right] + \Gamma_s \bar{\rho}_s E_s \tag{54}$$

where

$$\eta_\xi = 1 - \frac{\bar{\rho}_{\xi 0}}{\bar{\rho}_\xi}. \tag{55}$$

The parameters $c_{\xi 0}$, s_ξ and Γ_ξ are specified constants which are intrinsic properties of the C_ξ.

By using eqn (52), eqn (50) can be rewritten to obtain

$$\frac{\partial F}{\partial \bar{\phi}_s} \equiv \mathscr{F} = \frac{P_{sb} - P_s}{\rho_s} - \Psi_{sg} \frac{\partial g}{\partial \bar{\phi}_s}. \tag{56}$$

When inverted, this relation becomes

$$\bar{\phi}_s = \mathscr{F}^{-1}(\Omega) \tag{57}$$

where

$$\Omega = \frac{P_{sb} - P_s}{\rho_s} - \Psi_{sg} \frac{\partial g}{\partial \bar{\phi}_s}. \tag{58}$$

In the work of Herrmann[15], the reciprocal of ϕ_s is called the distention of the solid and is denoted as α. In his work a relation is specified between the intrinsic bulk pressure and the distention. This relation describes the elastic range of a dry solid and is called the elastic P–α function. For a dry porous solid eqn (27) requires $P_s = 0$. Under conditions of hydrostatic compression, the second term in Ω is a constant, and the elastic part of the volume fraction of the solid is a function of the intrinsic bulk pressure. Thus eqn (57) is a generalization of Herrmann's P–α function and constitutes a mixing rule for the interaction of the solid and the pore fluid. It applies not only to dry porous solids under hydrostatic loading conditions, but also to solids containing pore fluids and subject to deviatoric as well as hydrostatic loads. Most importantly, eqn (57) implies that *once the elastic P–α function is established for the dry solid under hydrostatic loading conditions, the same function is valid for all saturation and loading conditions.* By noting eqn (27), eqn (57) also supports Nur and Byerlee's conclusion that under hydrostatic loading conditions the $\bar{\phi}_s$ cannot change unless the pressure difference $P_{sb} - P_f$ is changed.

In the present work the following form, suggested by Herrmann, will be chosen to represent eqn (57):

$$\frac{\tilde{\phi}_{sm} - \tilde{\phi}_s}{\tilde{\phi}_{sm} - \phi_{s0}} = \left(\frac{\Omega_m - \Omega}{\Omega_m}\right)^n \tag{59}$$

where $\tilde{\phi}_{sm}$, Ω_m and n are specified constants. This relationship is assumed to hold for $0 \leqslant \Omega \leqslant \Omega_m$. For $\Omega > \Omega_m$, $\tilde{\phi}_s = 0$.

The elastic deviatoric response of the solid is given by

$$g = g_0 + g_1 \tilde{\phi}_s \tag{60}$$

and

$$\rho_{s0} \Psi_{sg} = G_0 \Lambda + \frac{1}{2} G_1 \Lambda^2. \tag{61}$$

These assumptions also define the deviatoric terms in eqn (58), and give rise to a dilatant behavior in the solid provided $g_1 \neq 0$. Under these conditions even when the pressure is held constant a change in Λ resulting from a distortion of the solid will result in a change in Ω. This will produce a change in $\tilde{\phi}_s$. *This coupling of the shear stiffness to the dilatancy behavior is an important consequence of the entropy inequality. It is included to ensure compliance with the second law of thermodynamics.*

Since from eqns (49) and (50)

$$\frac{1}{3} T_{kk} = \phi_s (P_s - P_{sb}) \tag{62}$$

the mechanical description of the elastic response of the mixture is complete. The intrinsic properties of each of the constituents have been defined, and the mechanical mixing rules, eqns (59) and (60), have also been defined.

The thermal mixing rule is specified by establishing relations for the terms $\dot{e}_\xi$. Since the present concern is the stress-wave behavior of this mixture which occurs on a rapid time scale, it is assumed that heat exchange between the constituents can be neglected. Therefore

$$\dot{e}_\xi = 0. \tag{63}$$

Before proceeding with the description of the inelastic response of the solid, one additional relation will be noted. If the sound speed in the dry solid is computed as $c_e^2 = -\partial T_{kk}/\partial \rho_s$ evaluated at zero load, then it can be shown that

$$\left(\frac{c_{s0}}{c_e}\right)^2 = 1 + \frac{\tilde{\phi}_{sm} - \phi_{s0}}{\Omega_m} n c_{s0}^2. \tag{64}$$

Specification of the remaining response functions of the mixture is keyed to the entropy inequality. By incorporating the thermal mixing rule, eqn (63), into the inequality, eqn (51),

and by requiring the remaining terms to separately satisfy the resulting relation, the following conditions are obtained:

$$T_{ij}^{e'}\left[\frac{1}{2}(\mathscr{L}_{ij}+\mathscr{L}_{ji})-\dot{\varepsilon}_{ij}'\right]\geqslant 0 \tag{65}$$

$$-T_{kk}(\dot{\phi}_s-\dot{\bar{\phi}}_s)\geqslant 0 \tag{66}$$

$$-T_{kk}^{d}\frac{\dot{\rho}_s}{\rho_s}\geqslant 0 \tag{67}$$

and

$$T_{ij}^{d'}(\mathscr{L}_{ij}+\mathscr{L}_{ji})\geqslant 0. \tag{68}$$

The first of these conditions can be simplified by substitution of eqns (48) and (61)

$$(\mathscr{L}_{ij}+\mathscr{L}_{ji})\varepsilon_{ij}'\geqslant \dot{\Lambda} \tag{69}$$

where it has been assumed

$$G_0+G_1\Lambda>0. \tag{70}$$

In the elastic range eqn (15) holds, and eqn (69) is satisfied identically. In the plastic range eqn (69) can be satisfied by limiting the deviatoric component $T_{ij}^{e'}$ so that

$$T_{ij}^{e'}T_{ij}^{e'}\leqslant\frac{2}{3}Y^2 \tag{71}$$

where Y is a specified yield criterion. To enforce this yield condition the $T_{ij}^{e'}$ are kept within the yield surface by requiring $\dot{\varepsilon}_{ij}=(\gamma/2)(\mathscr{L}_{ij}+\mathscr{L}_{ji})$ where $0\leqslant\gamma\leqslant 1$. When $T_{ij}^{e'}$ falls within the yield surface $\gamma=1$ else the value of γ is adjusted so as to keep $T_{ij}^{e'}$ on the yield surface.

The following expression for Y is chosen when the solid is subjected to compressive loads; that is, when T_{kk} is negative:

$$Y=y_0-y_1\exp\left[y_2\frac{(1/3)T_{kk}}{\phi_s}-y_3(\phi_s-\bar{\phi}_s)\right]. \tag{72}$$

The y_is are specified constants. When T_{kk} is positive

$$Y=y_0-y_1. \tag{73}$$

Here it is assumed that the shear strength of the solid matrix is sensitive to the spherical component of the configurational stress T_{kk}. Equations (27) and (62) show that T_{kk} is affected by the pore pressure. The degradation of shear strength by pore pressure is an important phenomenon in fluid saturated porous solids. It is also assumed the solid matrix exhibits an ability to work harden. To account for this Y is a function of the plastic volume fraction $\phi_s-\bar{\phi}_s$.

By substitution of eqn (62), inequality (66) becomes

$$\frac{P_{sb}-P_s}{\rho_s}(\dot{\phi}_s-\dot{\bar{\phi}}_s)\geqslant 0. \tag{74}$$

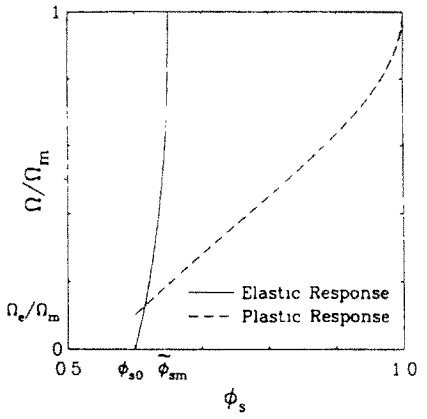

Fig. 1. Pore-compaction behavior of the solid.

In the elastic range of the solid, this inequality is satisfied identically because $\dot{\phi}_s = \dot{\tilde{\phi}}_s$. When the plastic volume fraction changes, it must change according to rules which ensure that inequality (74) is satisfied. As with the elastic deviator strains, the change in the plastic volume fraction will be controlled by a yield condition. It is required

$$-\Omega_e \leqslant \frac{P_{sb} - P_s}{\rho_s} \leqslant \Omega_i \tag{75}$$

where, following the form suggested by Herrmann

$$\left(\frac{\Omega_m - \Omega_i}{\Omega_m - \Omega_e}\right)^2 = \frac{1/\phi_s - 1}{1/\phi_{s0} - 1}. \tag{76}$$

The parameters Ω_m and Ω_e are positive constants. It is intended that the same values for Ω_m be used in this relation and in eqn (59). These conditions hold until $\phi_s = 1$ and $(P_{sb} - P_s)/\rho_s = \Omega_m$ after which $(P_{sb} - P_s)/\rho_s$ can again increase in magnitude.

These relations are illustrated in Fig. 1 for the situation when the plastic volume fraction is zero. Equation (59) is labelled the elastic response, and eqn (76) is labelled the plastic response. When, for example, the value of Ω increases and attempts to move the material response outside the envelope formed by eqn (76), the plastic volume fraction changes so as to shift the elastic response curve to the right and contain the elastic response within the envelope.

The remaining inequalities to be satisfied are given by relations (67) and (68). The specification of the dissipative stresses to achieve this will be discussed in the section on numerical methods.

4. THE EXPERIMENT AND PARAMETER SELECTION

To test the utility of the theory derived in the last two sections, results of numerical wave propagation calculations will be compared to data collected from a field test named the ONETON experiment. As discussed earlier, this experiment involved the detonation of a charge of high explosive buried in an ashfall tuff. The reports of Smith[13, 19] give a complete description of this experiment, and the limited description given here will only serve to provide continuity to the present work.

The site of the experiment was surveyed extensively. No faults or fractures were found either before or after the experiment. The structure of the formation was reasonably isotropic, and originally was believed to be saturated with water to about 95–98% of the pore volume. The error on the reported saturation level was sufficient to allow for the possibility of 100% saturation. It is generally believed among the people who fielded this

experiment that the water content was higher than the average of the reported values. The saturation level used in these calculations is 98.1%.

A 907 kg spherical charge of TNT was buried in this formation by first digging a tunnel access which was closed with grout prior to detonation. Detonation was initiated at a location labelled the "working point", the geometric center of the charge. Several types of gages were also placed in bore holes which were then filled with grout. These gages were of three types, ytterbium piezoresistive-stress gages encased in a fluid cell, fluid-filled pancake and toadstool stress gages, and piezoresistive accelerometers. These gages measured radial and hoop stresses as well as radial accelerations following detonation.† A system of pipes in the access tunnel were also used to measure the residual pressure within the explosively-formed cavity.

After the test a "mineback" procedure was used to recover and inspect the gages and to measure the cavity radius. This operation revealed a spherically-symmetric cavity and the absence of fractures within the surrounding material.

Cored material taken from a variety of bore holes was tested for material properties. The results of these tests are summarized by Butcher and Chavez[20]. These data were used to determine the material parameters used for the calculation in this report.

The value of the mixture mass density, as noted earlier, is slightly higher than the originally reported value of $2003\,\mathrm{kg\,m^{-3}}$. The value used is

$$\rho_0 = 2009\,\mathrm{kg\,m^{-3}}. \tag{77}$$

The value of the initial intrinsic mass density of the tuff is

$$\tilde{\rho}_{s0} = 2530\,\mathrm{kg\,m^{-3}}. \tag{78}$$

This is also known as the mineral density of the solid. The mass density of the dry distended tuff is

$$\rho_{s0} = 1680\,\mathrm{kg\,m^{-3}} \tag{79}$$

corresponding to a void volume of 34%. The intrinsic mass density of the water is

$$\tilde{\rho}_{f0} = 998\,\mathrm{kg\,m^{-3}}. \tag{80}$$

The intrinsic bulk sound speeds of the mineral and the water are

$$c_{s0} = 3.2\,\mathrm{km\,s^{-1}} \tag{81}$$

and

$$c_{f0} = 1.9\,\mathrm{km\,s^{-1}}. \tag{82}$$

The intrinsic non-linear stiffness coefficients in eqns (53) and (54) are

$$s_s = 1.13 \tag{83}$$

† The accuracy of this type of stress measurement is subject to debate. Smith[13] addresses this question in his experimental work; however, no clear answers seem to be available. The presence of the bore hole within the rock, the type of grout used to fill the hole after emplacement of the gage package, and the method of coupling the gage within the package to the surrounding grout can strongly affect the gage performance. Generally, it is believed that gages which are oriented to measure normal stresses in the radial direction are much more accurate than identical gages which are oriented to measure normal stresses in the hoop direction.

and

$$s_f = 1.58. \tag{84}$$

The values of the Grüneisen parameter used in these relations are

$$\Gamma_s = 0.2 \tag{85}$$

and

$$\Gamma_f = 0.0. \tag{86}$$

A value of $2.01\,\mathrm{km\,s^{-1}}$ was reported for the sound speed in the *in situ* material. This value was multiplied by the square root of the ratio ρ_0/ρ_{s0} to arrive at the sound speed for the dry distended solid as given in (64). Thus

$$c_e = 2.19\,\mathrm{km\,s^{-1}}. \tag{87}$$

It is assumed at acoustic pressures that the presence of the water within the pores contributes to the mass of the mixture, but does not contribute to the stiffness.

The parameters for the onset and completion of crushing of the solid during hydrostatic loading are

$$\rho_{s0}\Omega_e = 10\,\mathrm{MPa} \tag{88}$$

and

$$\tilde{\rho}_{s0}\Omega_m = 4\,\mathrm{GPa}. \tag{89}$$

These values indicate that initially this tuff is quite easily crushed; however, substantial pressures are required to remove the final amount of porosity in a drained sample.

The value of n in eqn (59) is

$$n = 2.5. \tag{90}$$

The shear modulus of the solid is reported to be 3.13 GPa in the *in situ* material and 10.3 GPa in the fully-compacted material. This modulus is assumed to be constant during distortion of the solid. Thus

$$G_0 = 10.3\,\mathrm{GPa} \tag{91}$$

$$G_1 = 0 \tag{92}$$

$$g_0 = -1.07 \tag{93}$$

$$g_1 = 2.07. \tag{94}$$

The shear strength of the solid is reported to range from an *in situ* value of 8 MPa to a maximum value of 39 MPa achieved under elevated confining pressures. Thus the constants for eqn (72) are

$$y_0 = 39\,\mathrm{MPa} \tag{95}$$

and

$$y_1 = 31\,\text{MPa}. \tag{96}$$

The exponential form of eqn (72) was originally fit to the core data using the term $\frac{1}{3}T_{kk}y_2$ in the argument of the exponential. The value of the constant used was $3.1\,\text{GPa}^{-1}$. This fit represents the behavior of the solid during initial loading of the sample. The effect of subsequent unloading is not known. There are an infinite number of sets of y_2 and y_3 which will approximate this initial loading behavior; however, since the magnitude of T_{kk} will decrease during unloading and the magnitude of $\phi_s - \tilde{\phi}_s$ will not, the unloading behavior will differ for each choice. Calculations will show that the final radius of the explosively-formed cavity is sensitive to this choice. The choice used in the work is based upon this criteria. The assumed values are

$$y_2 = 1.59\,\text{GPa}^{-1} \tag{97}$$

and

$$y_3 = 112.5. \tag{98}$$

Upon unloading after passage of the initial shock pulse, these parameters will result in a 25% loss of peak strength in the material at close range to the working point.

5. NUMERICAL METHODS

The structure of this theory consists of a set of balance equations for mass, momentum and energy, a set of constitutive equations for the intrinsic material behavior, and a set of mixing rules for the volume fractions and the heat exchange. The mixture balance of mass and balance of momentum equations, eqns (10) and (28), are identical to their counterparts for conventional theories of single continua. Because of this structure, the theory can be incorporated into a conventional wave propagation code. Lagrangian codes are particularly adaptable to these types of modifications since they do not require specification of new convection schemes for the additional variables appearing in the constitutive formulation.

The wave propagation code WONDY V[18] can generate solutions to one-dimensional problems in either plane, cylindrical or spherical coordinates. Its basic architecture consists of an explicit finite-difference scheme for solving the mass and momentum equations to obtain new material positions and velocities at a particular material point. This information is then introduced into the material response subroutine where the constitutive equations and the energy balance equations are solved. This produces new values for the stresses at that material point. The process is then repeated for neighboring material points until all of them have been updated to the new time.

The numerical-methods problem is therefore reduced to generating a solution technique for the constitutive and energy equations to calculate the required stresses at the new time. The method chosen is to transform these equations into a set of ordinary differential equations and use an auxiliary numerical integrator to obtain the required information. The system is reduced to six equations in the variables ϕ_s, $\tilde{\phi}_s$, E_s, E_f, ε'_{rr}, and $\varepsilon'_{\theta\theta}$ where r and θ denote the radial and hoop directions in the spherically symmetric problem. Given that these quantities are known at a particular time, the auxiliary integrator requires the values of their time derivatives.

The first step in this process is to linearly interpolate the mixture mass density ρ between the old time and the new time. This defines the mass density and its time derivative over the required time interval. The partial mass densities ρ_ξ are also defined through eqn (11). The volume fraction of the pore water can be computed by first assuming absence of void so that $\phi_f = 1 - \phi_s$. The intrinsic mass densities are then computed from eqn (6). If $\bar{\rho}_f \leqslant \bar{\rho}_{f0}$, then void exists, and ϕ_f is recomputed by using $\bar{\rho}_f = \bar{\rho}_{f0}$. Next the pressures P_f

and P_{sb} are computed from eqns (53) and (54). Equations (27), (58) and (59) can now be used to estimate a value for the elastic volume fraction of the solid, $\bar{\phi}_{se}$. In general this value will not be equal to the stored value of $\bar{\phi}_s$. Because the solution procedure, eqn (27) is not satisfied identically. These two values for the elastic volume fraction will be used to compute one of the required derivatives by using the following relationship:

$$\frac{d}{dt}\bar{\phi}_s = -\frac{1}{\tau}(\bar{\phi}_s - \bar{\phi}_{se}). \tag{99}$$

A small value of the relaxation time τ is chosen so that $\bar{\phi}_s$ and $\bar{\phi}_{se}$ are approximately equal throughout the calculation. It is not intended that eqn (99) have any physical interpretation. It is merely a computational convenience.

If plastic pore collapse occurs, the required time derivative for the volume fraction of the solid is computed by using inequality (75). In this case another evolution equation is used so that

$$\frac{d}{dt}(\phi_s - \bar{\phi}_s) = -\frac{1}{\tau\Omega_{lim}}\left(\frac{P_{sb} - P_s}{\rho_s} - \Omega_{lim}\right) \tag{100}$$

where Ω_{lim} assumes values of $-\Omega_e$ and Ω_l as prescribed by eqn (75). The derivatives of the two elastic strains are also computed by evolution equations similar to eqn (100) where the limiting conditions are specified by the yield condition, eqn (71). The same value of τ is used in all the evolution equations. For the computations included in this work $\tau = 1\ \mu s$ produced accurate solutions of the constitutive equations. Smaller values of τ resulted in identical solutions, but at the cost of additional computational time. The procedure is completed by computing the required derivatives for the internal energies from the energy balance relations (29) and (30).

In most wavecodes, artificial viscosity is used to "stabilize" the numerical solutions in the neighborhood of shock waves. In the WONDY code this term has two parts: one is linear and the other is quadratic in $\dot{\rho}$. Both terms satisfy inequality (67). In these computations, the sum of these terms is set equal to T^d_{kk}. $T^{d'}_{ij}$ is set equal to zero. Thus the effects of shock heating, which are introduced through this artificial-viscosity term, are experienced totally by the solid.

6. RESULTS AND COMPARISON TO EXPERIMENT

In Sections 2 and 3 a model was developed for wet tuff. In Section 4, motivated by a particular field experiment, a set of constitutive parameters were chosen. By using the numerical procedure outlined in Section 5, stress wave calculations have been obtained for that experiment. In this section, these results will be discussed and compared to the data.

In the calculation a spherical charge of TNT is detonated at the geometric center or "working point" of the problem. The charge is 0.51 m in radius. It is characterized by a Jones–Wilkins–Lee (JWL) equation of state[21]. Wet tuff forms a thick hollow sphere surrounding and in contact with the charge. It has an outer diameter of 20 m. This allows computation to a 20 ms problem time before waves of significant amplitude can travel from the working point to the outer boundary and return to the region of interest. Within this time, this finite sphere of tuff approximates an infinite medium.

The gages fielded in the experiment are listed in Table 1. This table lists the quantity measured by the gage and its distance or range from the working point. The leading digits in the gage name indicate the bore hole into which the gages were positioned, and the letters indicate the gage type; either fluid-coupled ytterbium (YFC), toadstool (TS), pancake (PC) or accelerometer (AC).

It is instructive to first examine and compare the gage records independently of the

Table 1. Field test gages

Gage	Type	Range (m)
1YFC	Radial stress	1.70
2YFC	Radial stress	2.03
4YFC	Radial stress	2.51
5YFC	Radial stress	3.72
5AC	Velocity	3.72
8YFC	Radial stress	5.27
8AC	Velocity	5.27
9TS1	Radial stress	5.16
9PC1	Hoop stress	5.32
9TS2	Radial stress	7.45
9PC2	Hoop stress	7.60
12YFC	Radial stress	7.63
12AC	Velocity	7.63

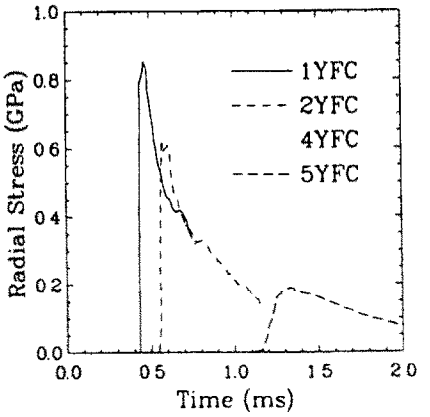

Fig. 2. Field-test data collected at close range.

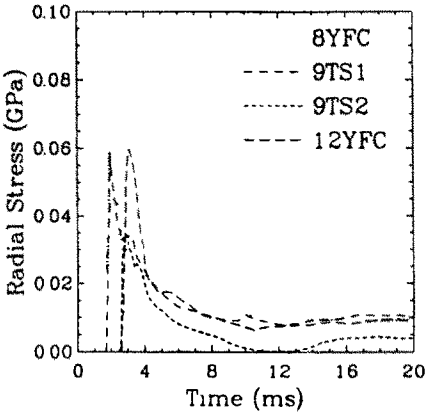

Fig. 3. Field-test data collected at long range.

calculations. Figures 2 and 3 contain the data from the gages which measured radial stress. In Fig. 2, four records of radial-stress measurements are compared over the first 2 ms after detonation. The data appears consistent and gives a clear indication of the decay of the stress pulse as it radiates outward from the working point. In Fig. 3 the remaining records of radial stress are compared on a more compressed time scale. These data show more scatter but with the exception of 12YFC, these records also fall along a common decay curve.

Figures 4–9 contain comparisons of the calculation to these data. Considering the scatter which is typical of data obtained from field tests, the comparisons are generally good. The comparisons to gages 1YFC, 2YFC and 4YFC are exceptionally good.

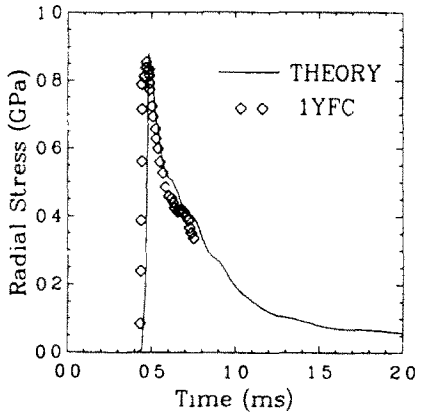

Fig. 4. Radial-stress comparison at 1.70 m range.

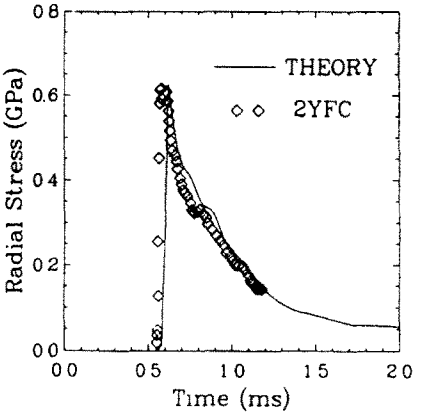

Fig. 5. Radial-stress comparison at 2.03 m range.

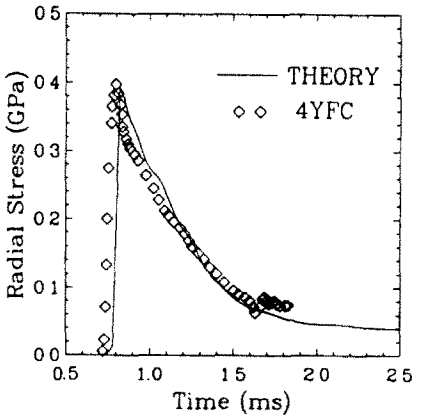

Fig. 6. Radial-stress comparison at 2.51 m range.

The late-time response of the calculations shown in Figs 8 and 9 have a greater amount of ringing than the data. This is probably due to the omission of any physical dissipative effects within the material response functions. The calculations also suggest that gages 12YFC and 9TS2 should have recorded nearly identical data. As noted earlier, 12YFC did not conform with the other gage records.

Beginning with Fig. 7, the calculations also exhibit a weak precursor wave at the lower leading edge of the shock front. This wave is a consequence of the transition of the solid from a partially-saturated medium to a fully-saturated medium during initial crushing of the solid matrix.

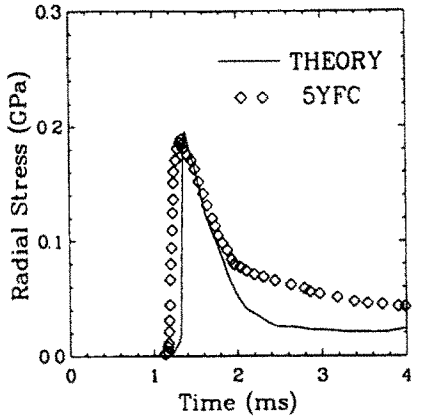

Fig. 7. Radial-stress comparison at 3.72 m range.

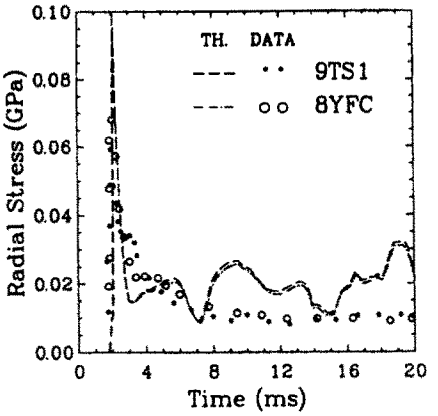

Fig. 8. Radial-stress comparison at 5.16 and 5.27 m range.

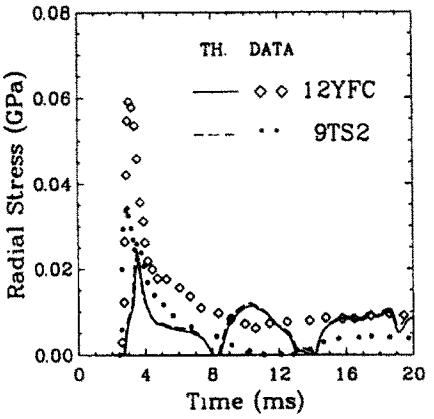

Fig. 9. Radial-stress comparison at 7.45 and 7.63 m range.

Comparisons of the calculation to the accelerometer data are contained in Figs 10–12. Again the comparisons are good with the exception of gage 12AC. This gage was paired with 12YFC in the same bore hole. The peaks of both gages are under-predicted by approximately 50%.

Comparison to the hoop-stress data is shown in Fig. 13. The gage record for 9PC2 suggests this gage went into a state of tension at 4.5 ms which could not be measured. The peak loads are under-predicted in the case of 9PC2 and over-predicted in the case of 9PC1. The calculation also predicts tension at both gage locations; however, 9PC1 registered only compressive loads.

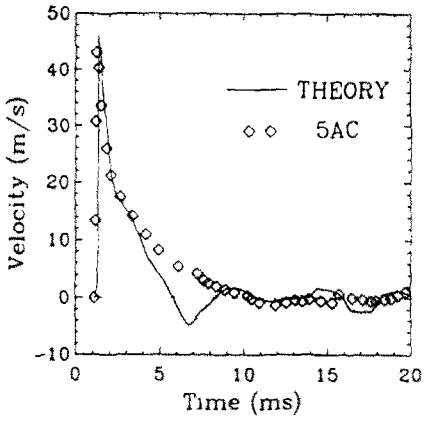

Fig. 10. Velocity comparison at 3.72 m range.

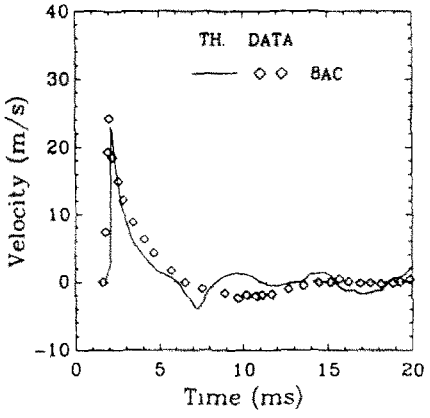

Fig. 11. Velocity comparison at 5.27 m range.

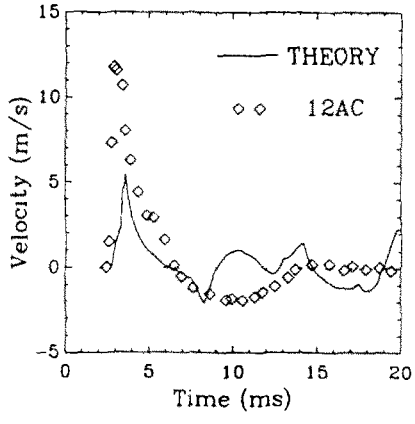

Fig. 12. Velocity comparison at 7.63 m range.

The calculation shows peak radial stresses of 10 GPa at the tuff–explosive interface. The resulting stress wave rapidly attenuates, and by the time it travels 1 m to the first stress gage, its amplitude has diminished to approximately 0.9 GPa. After 2.5 ms the stress wave has propagated about 6 m and attenuated to 0.06 GPa. Figure 14 is a plot of the computed radial and hoop stresses and the pore-fluid pressure vs Eulerian position at 2.5 ms. The development of a second stress pulse near the explosive cavity is evident. The accelerometer 5AC has moved to the 3.74 m point where the second stress pulse is about to intercept it. As illustrated in Fig. 10, this produces a small change in slope in both the calculation and the gage record at 2.5 ms. The influence of the second stress pulse upon

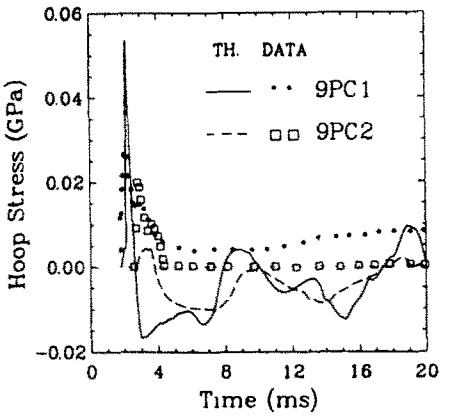

Fig. 13. Hoop-stress comparison at 5.32 and 7.60 m range.

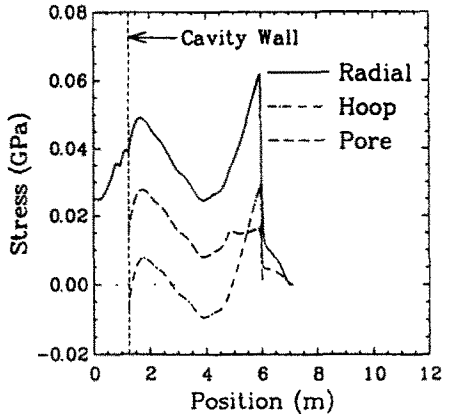

Fig. 14. Pore-fluid pressure and solid-matrix stresses at 2.5 ms.

the calculation is small because of the hardening effect introduced into the solid description through eqn (72). While the total load is still high at this point, the configurational load T_{kk} has dropped to a negligible value due to crushing of the pores followed by a partial release. In calculations where hardening is ignored the influence of this second pulse produces a prediction for gage 5AC which breaks to a nearly horizontal line at this point in time.

The inclusion of hardening in this model is also motivated by another consideration. Beginning a short time after detonation, the pressure within the explosive cavity was monitored, and eventually mining operations exposed the cavity so that its final radius could be measured. Both of these quantities are predicted by the calculation, and both comparisons are in poor agreement when the hardening effect is ignored; for example, the estimated cavity volume is twice as large as the measured volume. With the inclusion of hardening the displacement of the cavity wall is estimated to be 0.94 m compared to a measured value of 0.86 m, and the estimated cavity pressure is 21 MPa compared to a measured value of 23 MPa.

After 17.5 ms little motion remains within the tuff, and the stress configuration represents the long-term residual stress produced within the formation by the detonation. Figure 15 contains plots of the radial and hoop stresses and the pore-fluid pressure at this time. The stress cage is evident. An annular region of compressive stress is formed about the cavity. Due to spring back of the formation, the peak compressive hoop stress is greater than any other load at this time or at 2.5 ms. In addition, void has been crushed out of the formation to a range of 5.6 m from the working point.

For a period of days after detonation, water was observed to flow into the nearest open tunnel. This flow was thought to result from the pressure gradient induced into the pore fluid by the stress-cage effect.

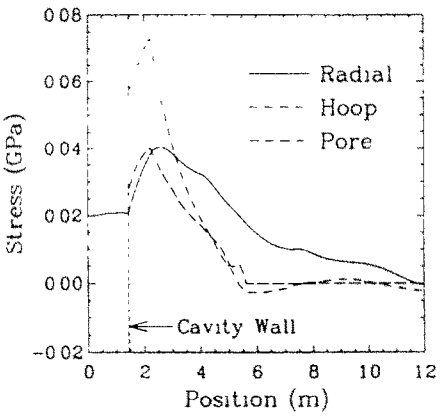

Fig. 15. Pore-fluid pressure and solid-matrix stresses at 17.5 ms.

7. SUMMARY

A theory for shock loading of wet tuff is derived. The theory is a generalization of the P–α model of Herrmann[15]. It contains an effective stress principle which differs from the original principle of Terzaghi[1]. Under conditions of hydrostatic loading, this effective stress principle corresponds to that proposed by Biot and Willis[3] and Nur and Byerlee[4]. Two important features of this theory are: the phenomena of dilatancy will occur whenever the shear modulus is specified as a function of the solid porosity; and the function linking the porosity of a dry porous solid to the hydrostatic confining load, the "P–α function", is universal to all saturation and loading conditions.

Thermodynamics is also given careful consideration in this work. The material response functions are linked to an equation-of-state or energy function, and the constraints imposed by the second law of thermodynamics are derived. Thus the response functions studied in this work describe material behavior which is continuous and either reversible or dissipative.

Finally the model is tested against stress-wave data obtained by detonating a spherical charge of TNT in a formation of partially-saturated tuff. It is demonstrated that good representations of radial and hoop stresses as well as velocities and displacements are obtained. The model is used to predict the formation of a residual stress pattern called a stress cage. It is also used to predict the residual pressure field within the pore water.

Acknowledgements—For various reasons there are always people who are of great help with any work, and whose names do not make it to the title page. I wish to thank M. E. Kipp for his generous assistance with the numerical aspects of this paper. Thanks are also given to C. W. Smith for numerous discussions about the field test ONETON.

REFERENCES

1. K. Van Terzaghi, Die Berechnung der Durchassigkeitsziffer des Tones aus dem Verlauf der hydrodynamischen Spannungserscheinungen, Sitzungsber. *Akad. Wiss. Wien Math. Naturwiss. Kl. Abt.* **2A**(132), 105–125 (1923).
2. A. Bedford and D. S. Drumheller, Theories of immiscible and structured mixtures. *Int. J. Engng Sci.* **21**, 863–957 (1983).
3. M. A. Biot and D. G. Willis, The elastic coefficients of the theory of consolidation. *ASME J. Appl. Mech.* **24**, 594–601 (1957).
4. A. Nur and J. D. Byerlee, An exact effective stress law for elastic deformation of rock with fluids. *J. Geophys. Res.* **76**, 6414–6419 (1971).
5. M. M. Carroll and N. Katsube, The role of Terzaghi effective stress in linearly elastic deformation. *J. Energy Res. Tech.* **105**, 509–511 (1983).
6. M. A. Biot, General theory of three-dimensional consolidation. *J. Appl. Phys.* **12**, 155–164 (1940).
7. A. Bedford and D. S. Drumheller, A variational theory of porous media. *Int. J. Solids Structures* **15**, 967–980 (1979).
8. A. Bedford and M. Stern, A model for wave propagation in gassy sediments. *J. Acoust. Soc. Am.* **73**, 409–417 (1983).
9. D. S. Drumheller and A. Bedford, A thermomechanical theory for reacting immiscible mixtures. *Archs Ration. Mech. Analysis* **73**, 257–284 (1980).

10. L. W. Morland, A simple constitutive theory for a fluid-saturated porous solid. *J. Geophys. Res.* **77**, 890–900 (1972).
11. S. K. Garg, Wave propagation effects in a fluid-saturated porous solid. *J. Geophys. Res.* **76**, 7947–7962 (1971).
12. S. K. Garg and A. Nur, Effective stress laws for fluid-saturated porous rocks. *J. Geophys. Res.* **78**, 5911–5921 (1973).
13. C. W. Smith, ONETON: a high-explosive containment experiment in wet tuff. Sandia National Labs, SAND84-1073 (1984).
14. M. H. Rice, R. G. McQueen and J. M. Walsh, Compression of solids by strong shock waves, *Solid State Physics* (Edited by F. Seitz), Vol. 6. Academic Press, New York (1958).
15. W. Herrmann, Constitutive equation for the dynamic compaction of ductile porous materials. *J. Appl. Phys.* **40**, 2490–2499 (1968).
16. B. D. Coleman and W. Noll, The thermodynamics of elastic materials with heat conduction and viscosity. *Archs Ration. Mech. Analysis* **13**, 167–184 (1963).
17. Y. B. Zel'dovich and Y. P. Raizer, *Physics of Shock Waves and High-temperature Hydrodynamic Phenomena.* Academic Press, New York (1967).
18. M. E. Kipp and R. J. Lawrence, WONDY V—a one-dimensional finite-difference wave propagation code. Sandia National Labs, SAND81-0930 (1981).
19. C. W. Smith, Residual stress fields—results from high-explosive field tests, *Proceedings of Second Symposium of Containment of Underground Nuclear Explosions*, Kirtland AFB, Albuquerque, New Mexico (Edited by C. W. Olsen). 2–4 August (1983).
20. B. M. Butcher and P. Chavez, private communication.
21. B. M. Dobratz, *LLNL Explosives Handbook—Properties of Chemical Explosives and Explosive Simulants.* Lawrence Livermore National Labs, UCRL-52997 (1981).